Electronic Supplementary Material (ESI) for Physical Chemistry Chemical Physics.
This journal is © the Owner Societies 2015

Supplementary Information

DNA-assisted photoinduced charge transfer between a cationic poly(phenylene vinylene) and a cationic fullerene

Youngil Park[1], Zhongwei Liu[2,3], Prahlad K. Routh[2,3], Cheng-Yu Kuo[1], Young-Shin Park[1], Hsinhan Tsai[1], Jennifer S. Martinez[4], Andrew P. Shreve[5], Mircea Cotlet[2,3,*] and Hsing-Lin Wang[1*]

[1]Chemistry Division, Los Alamos National Laboratory, Los Alamos, NM 87545; [2]Center for Functional Nanomaterials, Brookhaven National Laboratory, Upton, NY 11793; [3]Materials Science Department, Stony Brook University, Stony Brook, NY 11790; [4]Center for Integrated Technologies and Institute for Materials Science, Los Alamos National Laboratory, Los Alamos, NM 87545; [5]University of New Mexico, Albuquerque, NM 87131.

Details on spectroscopic measurements

UV-Vis spectra were measured with a Perkin Elmer Lambda 20 spectrophotometer, photoluminescence spectra with a Varian Cary Eclipse fluorimeter, dynamic light scattering with a Malvern Zetasizer. Fluorescence decays were measured by the time-correlated single photon counting (TCSPC) method using a Picoquant FluoTime 200 spectrometer combined with a solid state femtosecond laser system delivering 460nm pulses (85 fs pulse width at 8MHz), with an overall instrumental response function of 45 ps. A complete description of the system can be found in ref [1]. PL lifetimes were estimated by reconvolution of the measured PL decay with the instrumental response function and using a multiexponential function according to:

$$\tau_{ave} = (a_i \times \tau_i)/\sum_i (a_i \tau_i) \qquad \text{(s1)}$$

Proposed modified model for the quenching sphere of action

For nonlinear SV curves like that exhibited by C-PPV:ssDNA:C-C_{60} shown in Fig.3b and accompanied by nonlinear τ_{PL}(D)/ τ_{PL}(DA) vs [A] dependency (Fig.3b, red square and line, main text), the quenching sphere of action is an appropriate model[2]. This model assumes that there is no static quenching, instead an apparent static quenching component is attributed to the presence of the quencher near the emitter in a volume (sphere of action) where the probability of quenching following optical excitation is unity[2c, 3]. A general equation can be written for this model as follows

$$PL(D)/PL(DA) = [(1-f_a) + \frac{f_a}{(1+k_D)\times \exp(V[A])}]^{-1} \qquad \text{(s2)}$$

with $f_a = PL^a(D)/[PL^a(D) + PL^b(D)]$ representing the fraction of emitters available for quenching and V, the sphere of action volume (see SI for details on derivation of eq.4). For a SV curve exhibiting upward curvature, $f_a = 1$ (all emitters are available to be quenched) and eq. s2 becomes the classic formula describing the sphere of action model[3a, 3c]

$$PL(D)/PL(DA) = (1 + k_D) \times \exp(V[A]) \qquad \text{(s3)}$$

We analyzed the SV curve from Fig.3b by splitting it according to the acceptor concentration range in low (0-0.4 **μ**M) and intermediate (2) (0.5-0.8**μ**M) concentration regimes exhibiting upward curvature and a high concentration regime (3) (0.9-1.6**μ**M) with downward curvature (Fig.S5, SI). Distinction between low (1) and intermediate (2) regimes was done based on the $\tau_{PL(D)}/\tau_{PL(DA)}$ vs [Acceptor] dependency, that is, linear vs nonlinear, respectively. For the first two regimes, we assume $f_a = 1$ (all emitters available for quenching), and use eq. s3 to retrieve $k_D(1)=3.3\times10^{-5}\mu M^{-1}$ and $V(1)=1.05\mu M^{-1}$ and $k_D(2)=3.3\times10^{-5}\mu M^{-1}$and $V(2)=1.49\mu M^{-1}$, suggesting radii for the sphere of action of r(1)=75nm and r(2)=84nm, and very little or no dynamic quenching. For the high concentration regime the SV curve fitted with eq s2 provides $f_a(3)=0.9$, $k_D(3)=0.46\mu M^{-1}$ and $V(3)=2.07\mu M^{-1}$ which in turn provides a sphere of action radius of 94nm, values which suggest that at high acceptor concentration charge transfer is mostly dynamic in nature.
Eq.s2 can be derived according to ref [4], where the fractional accessibility, or the percentage of emitters available for quenching can be defined as

$$f_a = \frac{I_0^a}{I_0^a + I_0^b} = I_0^a / I^0 \quad \text{(s4)}$$

with

$$I^0 = I_a^0 + I_b^0 \quad \text{(s3)} \qquad \text{(s5)}$$

the total PL intensity in the absence of the quencher, composed of I_a^0 as the PL intensity from emitters available (accessible) for quenching, and I_b^0 as the PL intensity from emitters inaccessible for quenching. According to the quenching sphere of action model, the PL intensity in the presence of a quencher Q can be written[4]

$$I = \frac{I_0^a}{(1+k_{SV}[Q])exp(v[Q])} + I_0^b \quad \text{(s5)}$$

Combining eqs.s4-6 we obtain

$$\frac{I}{I^0} = (1 - f_a) + f_a/[(1 + k_{SV}[Q])exp(v[Q])] \quad \text{(s6)}$$

which is the equivalent of eq.s2

1. Xu, Z.; Tsai, H.; Wang, H.-L.; Cotlet, M., Solvent Polarity Effect on Chain Conformation, Film Morphology, and Optical Properties of a Water-Soluble Conjugated Polymer. *The Journal of Physical Chemistry B* **2010,** *114* (36), 11746-11752.
2. (a) Selmarten, D.; Jones, M.; Rumbles, G.; Yu, P. R.; Nedeljkovic, J.; Shaheen, S., Quenching of semiconductor quantum dot photoluminescence by a pi-conjugated polymer. *Journal of Physical Chemistry B* **2005,** *109* (33), 15927-15932; (b) Lee, P. P. S.; Ngai, T.; Huang, J. D.; Wu, C.; Fong, W. P.; Ng, D. K. P., Synthesis, characterization, biodegradation, and in vitro photodynamic activities of silicon(IV) phthalocyanines conjugated axially with poly(epsilon-caprolactone). *Macromolecules* **2003,** *36* (20), 7527-7533; (c) Wang, D. L.; Wang, J.; Moses, D.; Bazan, G. C.; Heeger, A. J., Photoluminescence quenching of conjugated macromolecules by bipyridinium derivatives in aqueous media: Charge dependence. *Langmuir* **2001,** *17* (4), 1262-1266.

3. (a) Lakowicz, J. R., *Principles of Fluorescence Spectroscopy*. 2004; Vol. 2nd Edition, p 238-264; (b) Campbell, K.; Zappas, A.; Bunz, U.; Thio, Y. S.; Bucknall, D. G., Fluorescence quenching of a poly(para-phenylene ethynylenes) by C-60 fullerenes. *Journal of Photochemistry and Photobiology a-Chemistry* **2012,** *249*, 41-46; (c) Geddes, C. D., Optical halide sensing using fluorescence quenching: theory, simulations and applications - a review. *Measurement Science & Technology* **2001,** *12* (9), R53-R88.

4. Chris, D. G., Optical halide sensing using fluorescence quenching: theory, simulations and applications - a review. *Measurement Science and Technology* **2001,** *12* (9), R53.

Supplementary Figures

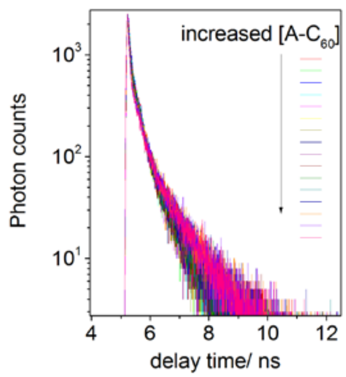

Figure S1. PL decays from C-PPV:A-C60 complex for various donor:acceptor molar ratios (defined in Fig.2b, main text). Arrow indicates increase in [A-C60]. PL excited at 460nm and detected at 580nm. C-PPV concentration was 0.3 μM.

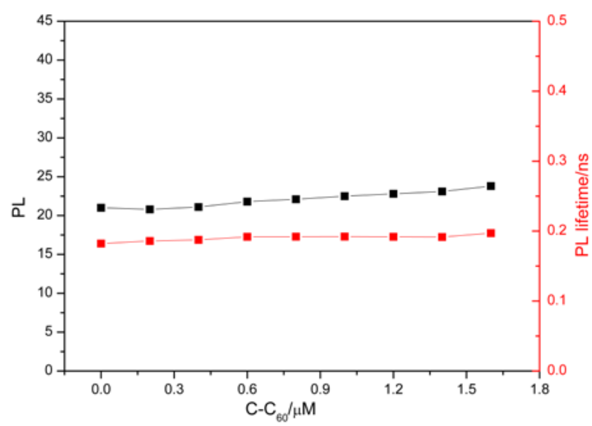

Figure S2. PL intensity (black squares and line) and PL lifetimes (red squares and line) of C-PPV vs added C-C_{60}. C-PPV concentration was 0.3 μM.

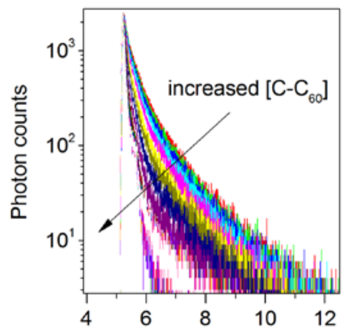

Figure S3. PL decays from C-PPV:ssDNA:C-C60 complex for various donor:acceptor molar ratios (defined in Fig.3b, main text), for a constant C:PPV:ssDNA molar ratio of 1:3. Arrow indicates increase in [C-C60]. PL excited at 460nm and detected at 580nm. C-PPV concentration was 0.3 μM.

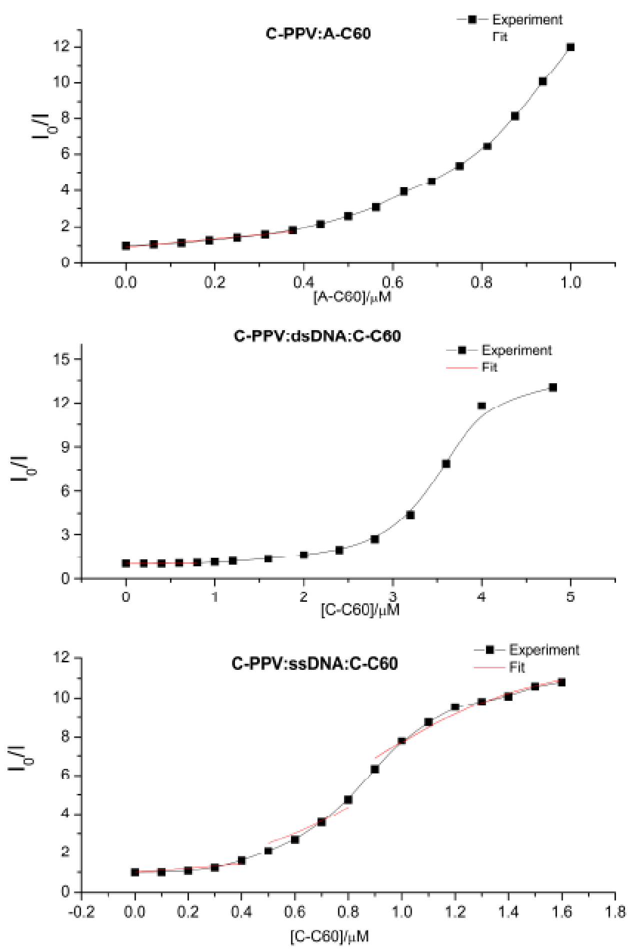

Figure S4. PL Stern-Volmer plot and fitting of (upper panel) C-PPV with increasing A-C_{60} concentration, C-PPV/dsDNA (middle panel) and C-PPV/ssDNA (lower) with increasing C-C_{60} concentration. Molar ratios for C-PPV:ssDNA and C-PPV:dsDNA were 1:3, in water and 1mM PBS, respectively. C-PPV concentration was 0.3 μM.

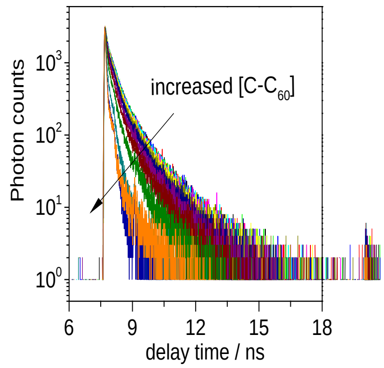

Figure S5. PL decays from C-PPV:dsDNA:C-C60 complex for various donor:acceptor molar ratios (defined in Fig.4b main text), for a constant C:PPV:dsDNA molar ratio of 1:3. PL excited at 460nm and detected at 580nm. C-PPV concentration was 0.3 μM. Arrow indicates increase in [C-C60]

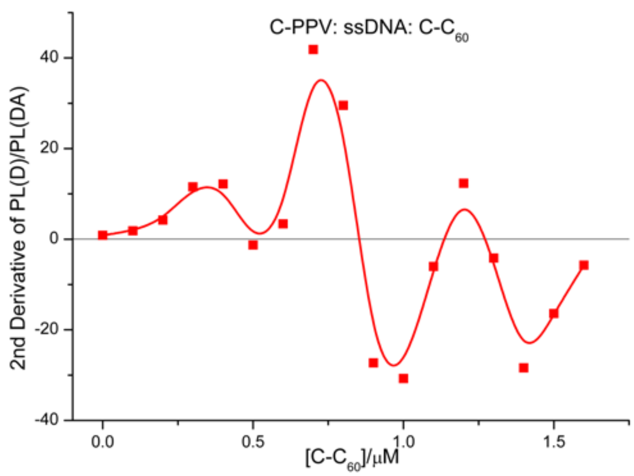

Figure S6. 2[nd] derivative of *PL(D)/PL(DA)* vs [C-C_{60}] dependency from Fig. 3b, main text, with an inflexion point at a C-C_{60} concentration of about 0.8μM.

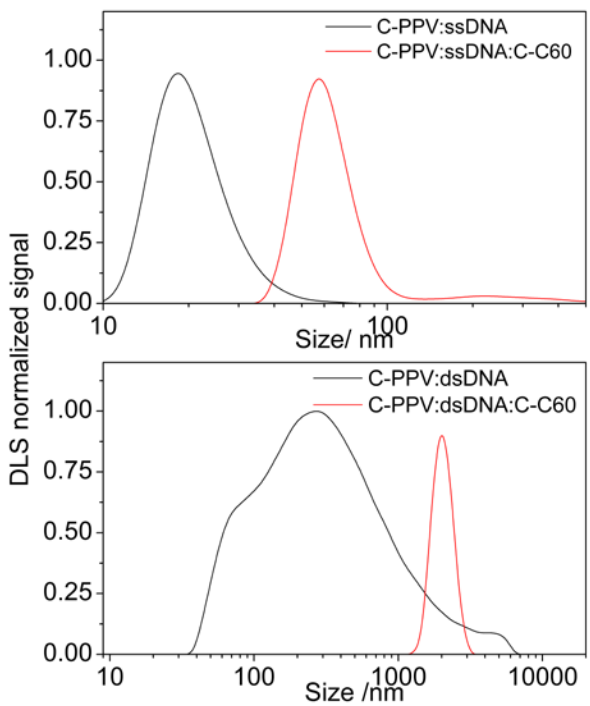

Figure S7. Dynamic light scattering measurements: upper panel, C-PPV:ssDNA (green line, water), C-PPV:ssDNA:C-C_{60} (black line, water); lower panel, C-PPV:dsDNA (green line, 1 mM PBS), C-PPV:dsDNA:C-C_{60} (black line, 1 mM PBS). Molar ratios: C-PPV:ssDNA, 1:3, C-PPV:ssDNA:C-C_{60}, 1:3:5, C-PPV:dsDNA 1:3, C-PPV:dsDNA:C-C_{60}, 1:3:15. C-PPV concentration was 0.3 μM.

Table S1: Surface zeta potential measurements. C-PPV was 0.3μM. Molar ratio of C-PPV:A-C_{60} was 1:3, C-PPV:ssDNA:C-C_{60}=1:3:5; C-PPV:dsDNA:C-C_{60}=1:3:15.

complex	**Zeta potential/mV**
C-PPV(in water)	+37.2
C-PPV (1mM PBS)	+11.0
C-C_{60} (in water)	+44.0
C-C_{60} (1mM PBS)	+20.0
C-PPV: A-C_{60} (water)	+29.7
C-PPV:ssDNA (in water)	-20.1
C-PPV:ssDNA:C-C_{60} (in water)	-5.19
C-PPV:dsDNA (1mM PBS)	-33.7
C-PPV:dsDNA:C-C_{60}(1mM PBS)	-16.6